

# Study on Turbulence Intensity Behavior under a Large Range of Temperature Variation

## **Authors:**

Junsik Lee, Jae-Hak Lee

*Date Submitted:* 2021-05-25

*Keywords:* wind tunnel, high-temperature, velocity fluctuation, turbulence intensity

## **Abstract:**

The turbulence intensity (TI) is defined as the ratio of fluctuation from the standard deviation of wind velocity to the mean value. Many studies have been performed on TI for flow dynamics and adapted various fields such as aerodynamics, jets, wind turbines, wind tunnel apparatuses, heat transfer, safety estimation of construction, etc. The TI represents an important parameter for determining the intensity of velocity variation and flow quality in industrial fluid mechanics. In this paper, computational fluid dynamic (CFD) simulation of TI alteration with increasing temperature has been performed using the finite volume method. A high-temperature—maximum 300 degrees Celsius (°C)—wind tunnel test rig has been used as the apparatus, and velocity was measured by an I-type hot-wire anemometer. The velocity and TI of the core test section were operated at several degrees of inlet temperatures at an air velocity of 20 m/s. The magnitude of TI has a relationship with boundary layer development. The TI increased as temperature increased due to turbulence created by the non-uniformities.

*Record Type:* Published Article

*Submitted To:* LAPSE (Living Archive for Process Systems Engineering)

*Citation (overall record, always the latest version):*

LAPSE:2021.0405

*Citation (this specific file, latest version):*

LAPSE:2021.0405-1

*Citation (this specific file, this version):*

LAPSE:2021.0405-1v1

*DOI of Published Version:* <https://doi.org/10.3390/pr8111403>

*License:* Creative Commons Attribution 4.0 International (CC BY 4.0)

Article

# Study on Turbulence Intensity Behavior under a Large Range of Temperature Variation

Junsik Lee and Jae-Hak Lee \*

Department of Aeronautical & Mechanical Engineering, Changshin University, Changwon-si, Gyeongsangnam-do 52833, Korea; jslee@cs.ac.kr

\* Correspondence: jhleepaul@cs.ac.kr; Tel.: +82-55-250-1352

Received: 19 October 2020; Accepted: 2 November 2020; Published: 3 November 2020



**Abstract:** The turbulence intensity (TI) is defined as the ratio of fluctuation from the standard deviation of wind velocity to the mean value. Many studies have been performed on TI for flow dynamics and adapted various fields such as aerodynamics, jets, wind turbines, wind tunnel apparatuses, heat transfer, safety estimation of construction, etc. The TI represents an important parameter for determining the intensity of velocity variation and flow quality in industrial fluid mechanics. In this paper, computational fluid dynamic (CFD) simulation of TI alteration with increasing temperature has been performed using the finite volume method. A high-temperature—maximum 300 degrees Celsius (°C)—wind tunnel test rig has been used as the apparatus, and velocity was measured by an I-type hot-wire anemometer. The velocity and TI of the core test section were operated at several degrees of inlet temperatures at an air velocity of 20 m/s. The magnitude of TI has a relationship with boundary layer development. The TI increased as temperature increased due to turbulence created by the non-uniformities.

**Keywords:** turbulence intensity; velocity fluctuation; high-temperature; wind tunnel

## 1. Introduction

The turbulence intensity (TI) represents a primary parameter for determining the intensity of wind velocity variation according to the ratio of fluctuation from the standard deviation of wind velocity to the mean value. The ratio reflects the importance of the element for wind-related phenomena such as buffeting, vortex-induced vibration, flutter, and galloping [1]. Many studies have been performed on TI for various fields in industrial fluid mechanics. Cook (2013) derived TI at varying altitudes for aircraft flight stability in a non-steady atmosphere for aerodynamics [2]. The longitudinal TI applied in jets was studied and the mean-flow and turbulence properties simulated by Dejoan et al. [3]. Barthelmie et al. researched detailed wind resources including TI for wind turbines and overviewed the state of the art in wind resource assessment with modeling and measurement techniques [4]. Moreover, TI has been the principal data in the production of electricity from wind energy [5]. The heat and mass transfer across the membrane considering TI was researched by Zhang [6], and Ahn et al. investigated the intrinsically unsteady heat transfer on the surface of a cylinder in crossflow in detail by numerical simulation as a function of the freestream TI [7].

In 2014, Silva et al. reviewed different TI interfacial layers, including the flow variable as velocity, and researched the flow dynamics which determine the growth, spreading, mixing, and reaction rates in many flows of engineering and natural interest [8]. Nishi et al. studied the environmental and boundary layer of a wind tunnel to control turbulence characteristics [9]. Kelberlau et al. estimated the TI with a continuous wave wind lidar [10], and Yang et al. studied the aerodynamic characteristics of a gurney flap in turbulence level (TI of 0.2%, 10.5%, and 19.0%) [11].

Basse studied TI with the friction factor from pipe flow measurements made in the Princeton Superpipe [12,13]. Wind tunnels are experimental devices to simulate certain flow conditions and to study the flow over objects of interest. The TI is one of the important parameters to estimate the flow quality inside the wind tunnel [14]. While setting boundary conditions for turbulence computational fluid dynamic (CFD) simulation, it is required to estimate the TI on the inlets [15]. L. Pareschi and M. Zanella proposed a novel numerical approach for computational fluid dynamics for aspace-homogeneous case, as temperature variation is taken into account and treated as an uncertain quantity [16].

Moreover, TI could be one of the most significant indicators indetermining the completeness of wind tunnel design and production. Despite this, few studies have been reported for the measurement of TI, considering the temperature increases. In this research, computational fluid dynamic (CFD) simulation of TI alteration with increasing temperature is used with the finite element method and experimental research under a certain freestream velocity. A high-temperature—up to 200 degrees Celsius (°C)—wind tunnel test rig has been designed as the apparatus, and velocity was measured by I-type hot-wire anemometer. The velocity and TI of the core test section were operated at several degrees of inlet temperatures at an air velocity of 20 m/s.

## 2. Computational Fluid Dynamics

In order to guarantee a reliable mode of estimation for TI in the wind tunnel, numerical simulations have to be investigated quantitatively. The analysis of velocity profiles according to temperature increases was carried out using the finite volume method using ANSYS Fluent [17].

The governing equations of computational fluid dynamics are continuity, momentum and energy conservation, as in Equations (1)–(3), respectively

$$\frac{\partial}{\partial x_i}(\rho x_i) = 0 \quad (1)$$

$$\frac{\partial}{\partial x_i}(\rho u_i u_j) = -\frac{\partial p}{\partial x_i} + \frac{\partial}{\partial x_j}(\tau_{ij} - \rho \overline{u_i u_j}) \quad (2)$$

$$\frac{\partial}{\partial x_i}(\rho C_p u_i T) = -\frac{\partial}{\partial x_i} \left( -k \frac{\partial T}{\partial x_i} + \rho C_p \overline{u_i T'} \right) \quad (3)$$

Where  $(i, j = 1, 2, 3)$  is the tensor notation of subscripts  $i$  and  $j$ , and  $u$  is the velocity vector,  $p$  is the pressure and  $T$  is the temperature, respectively.  $\rho$ ,  $C_p$  and  $k$  are the density, specific heat at constant pressure and coefficient of thermal conductivity. Moreover, Reynolds-averaged Navier–Stokes equations are used and  $\tau_{ij}$  is shown in Equation (4)

$$\tau_{ij} = \mu \left( \frac{\partial u_i}{\partial x_j} + \frac{\partial u_j}{\partial x_i} \right) \quad (4)$$

The standard k- $\epsilon$  model was applied for fully developed flow simulation with a two-dimensional (2D) steady state, considering the appropriate calculation. The transport equation for the standard k- $\epsilon$  model which was applied in numerical analysis is shown in Equation (5)

$$\begin{aligned} \frac{\partial}{\partial t}(\rho k) + \frac{\partial}{\partial x_i}(\rho k u_i) &= \frac{\partial}{\partial x_j} \left[ \left( \mu + \frac{\mu_t}{\sigma_k} \right) \frac{\partial k}{\partial x_j} \right] + G_k + G_b - \rho \epsilon - Y_M + S_k \\ \frac{\partial}{\partial t}(\rho \epsilon) + \frac{\partial}{\partial x_i}(\rho \epsilon u_i) &= \frac{\partial}{\partial x_j} \left[ \left( \mu + \frac{\mu_t}{\sigma_\epsilon} \right) \frac{\partial \epsilon}{\partial x_j} \right] + C_{1\epsilon} \frac{\epsilon}{k} (G_k + C_{3\epsilon} G_b) - C_{2\epsilon} \rho \frac{\epsilon^2}{k} + S_\epsilon \end{aligned} \quad (5)$$

where,  $G_k$  represents the generation of turbulence kinetic energy due to the mean velocity gradients, calculated as described in modeling turbulent production in the k- $\epsilon$  models.  $G_b$  is the generation of turbulence kinetic energy due to buoyancy, calculated as described in the effects of buoyancy on turbulence in the k- $\epsilon$  models.  $Y_M$  represents the contribution of the fluctuating dilatation in compressible

turbulence to the overall dissipation rate, calculated as described in the effects of compressibility on turbulence models.  $C_{1\varepsilon}$ ,  $C_{2\varepsilon}$ , and  $C_{3\varepsilon}$  are constants and  $\sigma_k$ ,  $\sigma_\varepsilon$  are the turbulent Prandtl numbers for  $k$  and  $\varepsilon$ , respectively.  $S_k$  and  $S_\varepsilon$  are user-defined source terms and the turbulent viscosity,  $\mu_t$ , is calculated by  $k$  and  $\varepsilon$ , as in Equation (6)

$$\mu_t = \rho C_\mu \frac{k^2}{\varepsilon} \quad (6)$$

$C_\mu$  is constant, and the model constant value  $C_{1\varepsilon} = 1.44$ ,  $C_{2\varepsilon} = 1.92$ ,  $C_{3\varepsilon} = 0.09$ ,  $\sigma_k = 1.0$ ,  $\sigma_\varepsilon = 1.3$  was accepted in this numerical simulation [18]. The boundary condition configured as the experimental condition with an inlet velocity of 20 m/s and an interior hot film probe region was applied. Figure 1 shows the modeling and number of 51,200 grids for computational simulation, and the boundary conditions and model parameters are listed in Table 1.

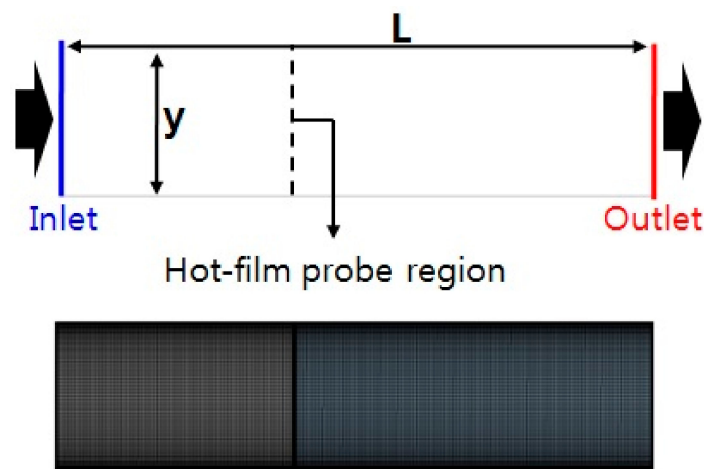
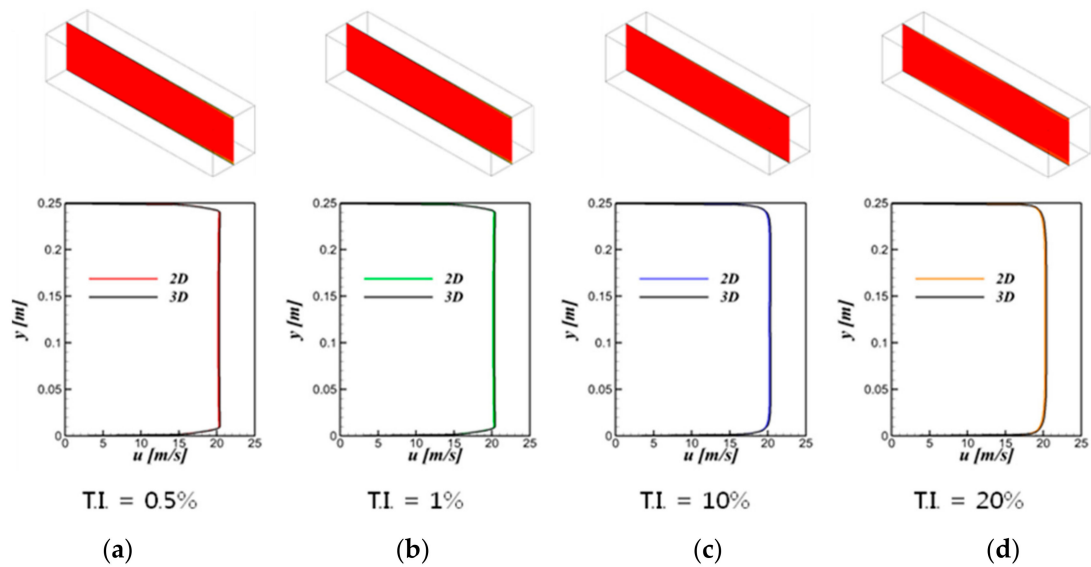


Figure 1. Schematic diagram of modeling and grid for simulation.

Table 1. The boundary conditions and model parameters.

Boundary Condition	Parameter
Inlet	Velocity inlet = 20m/s
Outlet	Pressure Outlet
Wall	No-slip and Adiabatic condition
Model and grid parameter	
Flow regime	2-D, Steady, Turbulent flow
Turbulence model	Standard k- $\varepsilon$ model
Grid type	Quadrilaterals
Number of grid	51200

Nevertheless, as the TI increases, the change in velocity distribution on the wall surface becomes noticeable and it is considered that the effect of TI is greater than the inlet temperature. For efficient calculation, numerical simulation was conducted to check whether the 2D and 3D result values were consistent, and the results are shown in Figure 2.



**Figure 2.** The comparison of 2D and 3D result for various turbulence intensities(TI); (a) 0.5%, (b) 1%, (c) 10%, (d) 20%.

Moreover, compared to TI, the velocity boundary layer is not affected by the inlet temperature change. Figure 3 shows the velocity profile of various TIs when increasing the temperature. The velocity gradient slightly decreases as the inlet temperature increases due to the Reynolds number decreasing according to the viscosity, which increases with temperature. The comparison result of the velocity profile for temperature increases in certain TIs is shown in Figure 4, and the velocity distribution near the boundary layer is relatively significant.

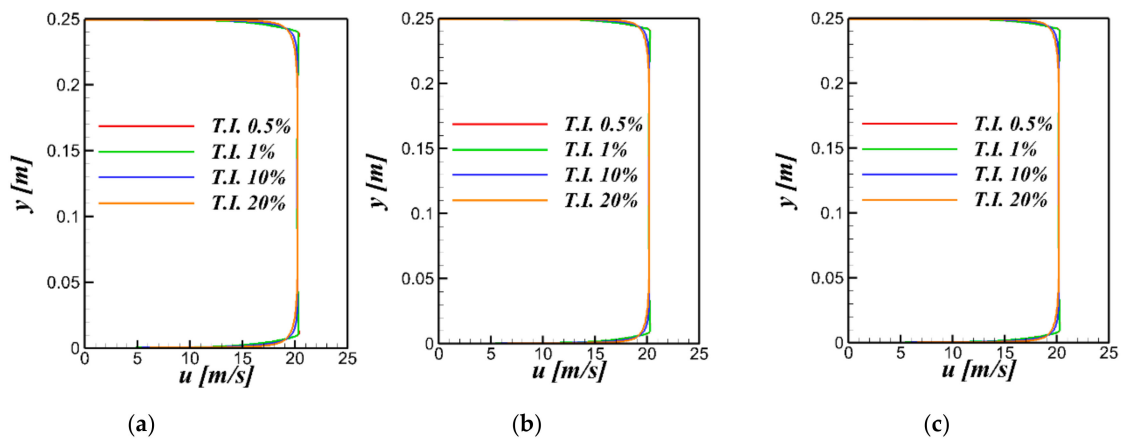


**Figure 3.** Velocity profile of various TI for the temperature; (a) 25, (b) 100, (c) 200 °C.

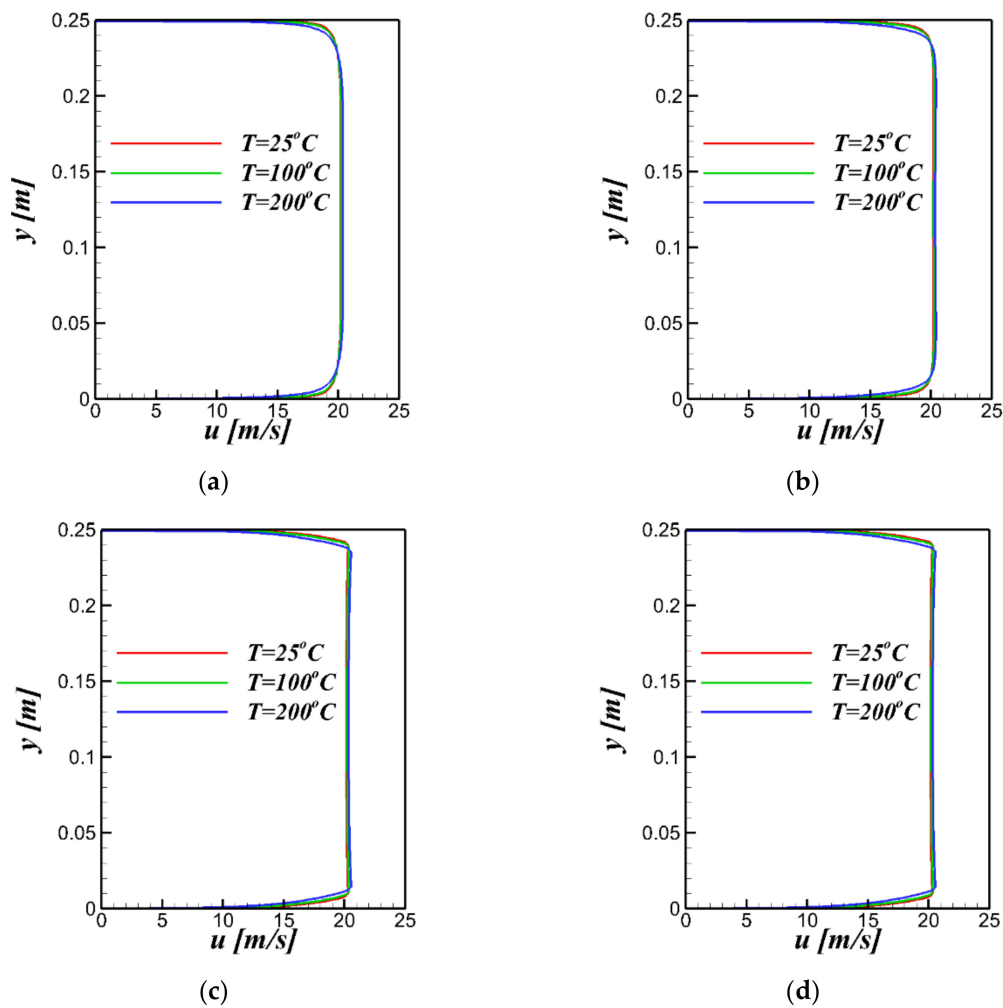


Figure 4. Velocity profile of temperature increases for the TI; (a) 0.5%, (b) 1%, (c) 10%, (d) 20%.

### 3. Experiments

Wind tunnels which can be regarded as applicable under high temperature have a maximum temperate of 300 °C, whereas nominal wind tunnels are used under normal ambient temperature. Figure 5 shows the schematic diagram of the comprehensive test equipment for a high-temperature wind tunnel including the test section where the TI is measured in certain conditions. The experiments provide a uniform free stream wind velocity of 20 m/s from a blower with a generation capacity of to the test section, passing 300 kW power consumption, with an electric heater through an inlet diffuser, with a honeycomb structure.

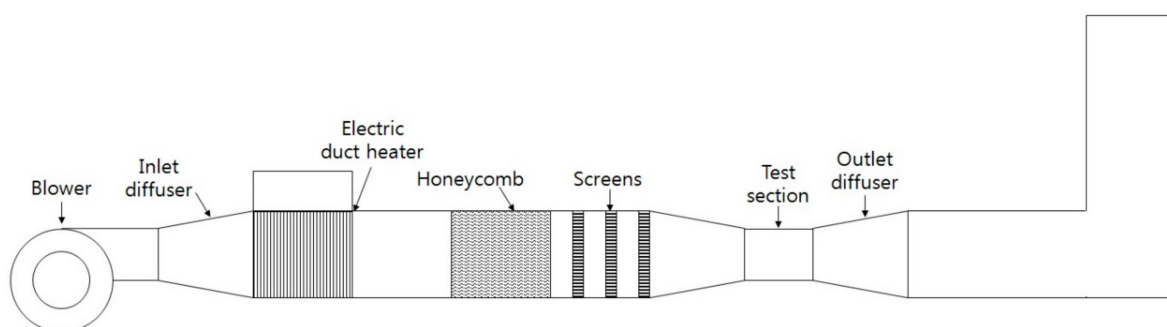


Figure 5. Schematic diagram of comprehensive test system of TI.

Figure 6 shows a schematic diagram of the test section with a square cross-sectional area of  $250 \times 250$  mm beneath the hot-wire probe. The 2D traverse device has been attached for measuring the velocity in the vertical(y) and horizontal (L) direction. The hot-wire measurement system consists of a sensor, a small electrically heated wire exposed to the fluid flow, and electronic equipment which performs the transformation of the sensor output into a useful electrical signal. The I-type hot-wire probe's (Model 1220 High Temperature Straight Probe, TSI) specifications are shown in Figure 7, which measured the velocity and TI for a maximum temperature of  $300\text{ }^{\circ}\text{C}$ .

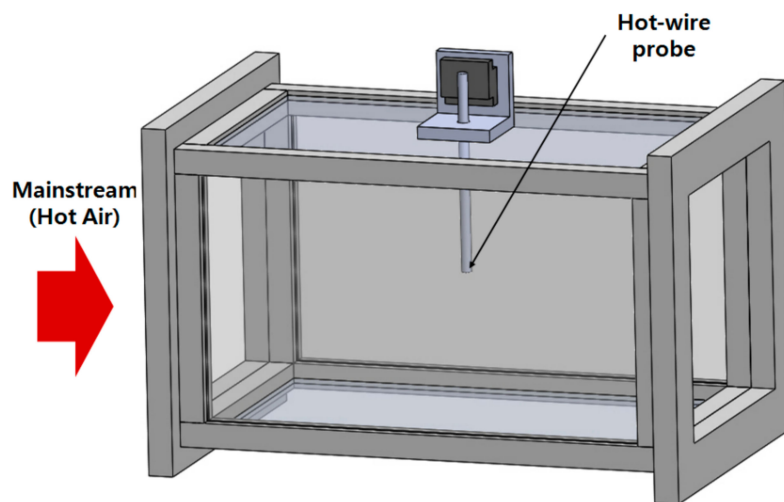


Figure 6. Schematic diagram of test section and hot wire probe.

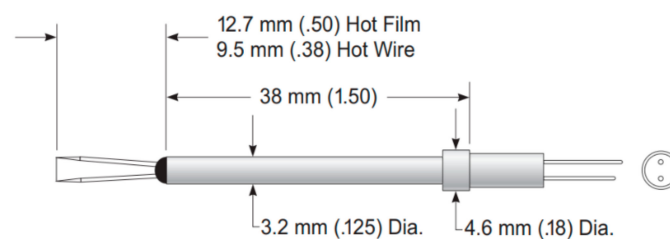


Figure 7. Specification of I-type hot wire probe.

#### 4. Result and Discussion

In order to examine the variation of TI according to the inlet flow temperature, the test was conducted by changing the inlet air flow temperature from atmospheric temperature to  $200\text{ }^{\circ}\text{C}$ . Figure 8 shows the result of the TI distribution in the longitudinal and horizontal direction. The temperature of inlet flow was  $25\text{ }^{\circ}\text{C}$ , and the velocity of the core of the main flow was  $20\text{ m/s}$ . In location at the middle of the wind tunnel, at which  $y = 125\text{ mm}$ , the TI was  $0.36\%$  and increased near the wall, as shown in CFD. In addition, the magnitude of TI has a relationship with boundary layer development. At  $x/L = 0.6$ , where boundary layer is developing, the TI was  $1.75\%$  at  $y = 5\text{ mm}$ . At  $x/L = 1$ , where the boundary layer is fully developed, it was  $3.5\%$  at the same altitude. The TI at the inlets for internal flows is generally dependent on the upstream history of the flow. Figure 9 shows the experiment results of the TI value according to the temperature increasing at the core of the wind tunnel test section at the free stream velocity of  $20\text{ m/s}$ . As temperature increased, the TI increased slightly. The measured average TI values are  $0.36\%$ ,  $0.6\%$ , and  $0.98\%$  at the temperature of  $25$ ,  $100$ ,  $200\text{ }^{\circ}\text{C}$ , respectively. Note that the experiment's TI values were very low for a lab-scale wind tunnel.

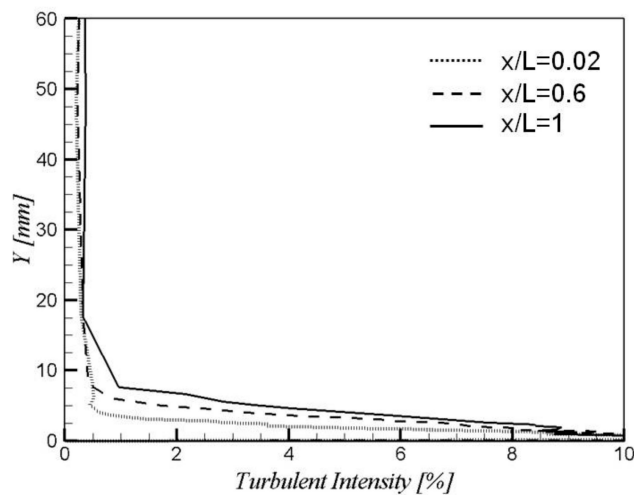


Figure 8. TI distribution of near the wall for wind velocity of 20 m/s.

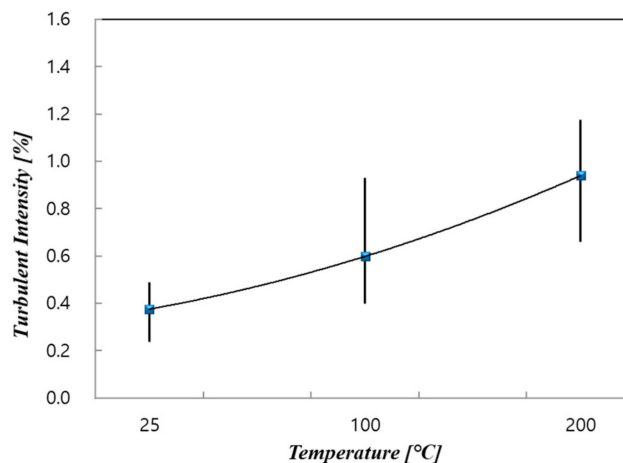


Figure 9. TI measurement increasing the temperature; 25 to 200 °C.

## 5. Conclusions

This study addresses the numerical simulation and experimental measurement of TI under an approaching free stream velocity with a high temperature gradient using a hot-wire anemometer. The influence of temperature is reflected in the TI values induced by the shear and its diffusion due to the turbulence generated. The stronger the shear becomes, the higher the level of turbulence with TI. The effect of free stream TI is more apparent on temperature change. The TI is slightly increased as temperature increases, and the magnitude of TI is related to boundary layer development due to the turbulence created by the non-uniformities.

**Author Contributions:** J.L. built up the research project, designed the experiments and performed investigation; J.-H.L. contributed to the search process, formal analysis and wrote the paper. All authors have read and agreed to the published version of the manuscript.

**Funding:** This work was supported by National Research Foundation of Korea (NRF) grant funded by the Korea government (MSIP; Ministry of Science, ICT & Future Planning) (No. 2017R1C1B5076422).

**Conflicts of Interest:** The authors declare no conflict of interest.

## References

1. Kimura, K. *Innovative Bridge Design Handbook*; Elsevier: Amsterdam, The Netherlands, 2016; pp. 37–48.
2. Cook, M.V. *Flight Dynamics Principles: A Linear Systems Approach to Aircraft Stability And Control*; Elsevier: Amsterdam, The Netherlands, 2013; pp. 4–444.



3. Dejoan, A.; Leschziner, M.A. Large eddy simulation of a plane turbulent wall jet. *Phys. Fluids* **2005**, *17*, 025102. [[CrossRef](#)]
4. Barthelmie, R.J.; Pryor, S.C. Meteorology and wind resource assessment for wind farm development. *Wind Energy Syst.* **2011**, *e28*, 3–27.
5. Sørensen, J.D.; Sørensen, J.N. Wind Energy Systems. *Woodhead Publ. Ser. Energy* **2011**, *1*, 46–111.
6. Silva, C.; Hunt, J.; Eames, I.; Westerweel, J. Interfacial Layers Between Regions of Different Turbulence Intensity. *Ann. Rev. Fluid Mech.* **2014**, *46*, 567–590. [[CrossRef](#)]
7. Zhang, L.Z. *Conjugate Heat and Mass Transfer in Heat Mass Exchanger Ducts*; Academic Press: Cambridge, MA, USA, 2013; pp. 181–232.
8. Ahn, J.; Sparrow, E.M.; Gorman, J.M. Turbulence intensity effects on heat transfer and fluid-flow for a circular cylinder in crossflow. *Int. J. Heat Mass Transf.* **2017**, *113*, 613–621. [[CrossRef](#)]
9. Nishih, A.; Miyagi, H.; Higuchi, K. A Computer-Controlled Wind Tunnel. In Proceedings of the 1st International Symposium on Computational Wind Engineering (CWE 92), Tokyo, Japan, 21–23 August 1993; pp. 837–846.
10. Kelberlau, F.; Neshaug, V.; Lønseth, L.; Bracchi, T.; Mann, J. Taking the Motion out of Floating Lidar: Turbulence Intensity Estimates with a Continuous-Wave Wind Lidar. *Remote Sens.* **2020**, *12*, 898. [[CrossRef](#)]
11. Yang, J.; Yang, H.; Zhu, W.; Li, N.; Yuan, Y. Experimental Study on Aerodynamic Characteristics of a Gurney Flap on a Wind Turbine Airfoil under High Turbulent Flow Condition. *Appl. Sci.* **2020**, *10*, 7258. [[CrossRef](#)]
12. Basse, N.T. Turbulence intensity and the friction factor for smooth- and rough-wall pipe flow. *Fluids* **2017**, *2*, 30. [[CrossRef](#)]
13. Basse, N.T. Turbulence Intensity Scaling: A Fugue. *Fluids* **2019**, *4*, 180. [[CrossRef](#)]
14. Mahta, R.D.; Bradshaw, P. Design rules for small low speed wind tunnels. *Aeronaut. J.* **1979**, *83*, 442–449.
15. Cattafesta, L.; Bahr, C.; Mathew, J. Fundamentals of Wind-Tunnel Design. *Exp. Tech. Fluid Dyn. Ther. Sci.* **2010**, 1–10. [[CrossRef](#)]
16. Pareschi, L.; Zanella, M. Monte Carlo stochastic Galerkin methods for the Boltzmann equation with uncertainties: space-homogeneous case. *J. Comput. Phys.* **2020**, *423*, 109822. [[CrossRef](#)]
17. Lee, J.S.; Seo, Y.M.; Jeong, C.H.; Kim, M.S.; Park, Y.G.; Ha, M.Y. Numerical analysis and design optimization of engine room to improve cooling performance for a mid-class excavator. *J. Mech. Sci. Technol.* **2019**, *33*, 3265–3275. [[CrossRef](#)]
18. ANSYS. *Fluent Theory Guide Release 15.0*; ANSYS, Inc.: Canonsburg, PA, USA, 2013; pp. 47–48.

**Publisher's Note:** MDPI stays neutral with regard to jurisdictional claims in published maps and institutional affiliations.



© 2020 by the authors. Licensee MDPI, Basel, Switzerland. This article is an open access article distributed under the terms and conditions of the Creative Commons Attribution (CC BY) license (<http://creativecommons.org/licenses/by/4.0/>).